Available online at www.sciencedirect.com
SCIENCE DIRECT®
Journal of Electron Spectroscopy and Related Phenomena 135 (2004) 105–112
JOURNAL OF ELECTRON SPECTROSCOPY and Related Phenomena
www.elsevier.com/locate/elspec

A high resolution photoemission study of surface core-level shifts in clean and oxygen-covered Ir(2 1 0) surfaces

M.J. Gladys [a], I. Ermanoski [a], G. Jackson [a], J.S. Quinton [a], J.E. Rowe [b], T.E. Madey [a,*]

[a] *Physics and Astronomy and Laboratory for Surface and Modification, Rutgers, The State University of New Jersey, 136 Frelinghuysen Road, Piscataway, NJ 08854-8019, USA*
[b] *Physics Department, North Carolina State University, Raleigh, NC 27695, USA*

Received 29 April 2003; received in revised form 3 February 2004; accepted 3 February 2004

Available online 18 March 2004

Abstract

High resolution soft X-ray photoemission electron spectroscopy (SXPS), using synchrotron radiation, is employed to investigate 4f core-level features of four differently-prepared Ir(2 1 0) surfaces: clean planar, oxygen-covered planar, oxygen-induced faceted, and clean faceted surfaces. Surface and bulk peak identifications are supported by measurements at different photon energies (thus probing different electron escape depths) and variable emission angles. Iridium $4f_{7/2}$ photoemission spectra are fitted with Doniach–Sunjic lineshapes. The surface components are identified with core levels positioned at lower binding energies than the bulk components, in contrast to previous reports of binding energy inversion on Ir(1 0 0) (1 × 1) and (5 × 1) surfaces. For clean planar Ir(2 1 0) three surface Ir $4f_{7/2}$ features are observed with core-level shifts of −765, −529, and −281 meV, with respect to the bulk; these are associated with the first, second and third layers of atoms, respectively, for atomically rough Ir(2 1 0). Adsorption of oxygen onto the planar Ir(2 1 0) surface is found to cause a suppression and shift of the surface features to higher binding energies. Annealing at $T \geq 600$ K in oxygen produces a faceted surface as verified by low energy electron diffraction (LEED). A comparison of planar and faceted oxygen-covered surfaces reveals minor differences in the normal emission SXPS spectra, while grazing emission spectra exhibit differences. The SXPS spectrum of the clean, faceted Ir(2 1 0) exhibits small differences in comparison to the clean planar case, with surface features having binding energy shifts of −710, −450, and −230 meV.

Keywords: Faceting; Iridium; Oxygen; Surface core-level shifts; Soft X-ray photoelectron spectroscopy; Low energy electron diffraction (LEED)

1. Introduction

There have been numerous reports of overlayer-induced faceting of transition metal substrates [1–17]; that is, an initially planar surface converts to a hill-and-valley structure when covered by monolayer films of gases and other metals. Metallic substrates that are known to form facets are atomically rough; they are morphologically unstable when covered with monolayer films of certain gases or other metals, followed by annealing. These surfaces include bcc W(1 1 1) [1–8] and Mo(1 1 1) [9–11], fcc (2 1 0) surfaces of Cu, Ni, Pt [12–14], and several vicinal (highly stepped) surfaces of Cu [15–17]. The most extensive studies have focused on W(1 1 1) surfaces.

Overlayer metals and adsorbates that induce faceting of the W(1 1 1) surface include Pt, Pd, Rh, Ir, Au, O, Cl, and Ru [1,2,4,6,7,18–20]. Ultrathin films that do not cause faceting of the substrate are Co, Ti, Gd, Ni, Cu, Ag, and Fe [6,7,21,22]. The facets are induced by covering the W(1 1 1) surface with a single monolayer of adsorbate, followed by heating to temperatures above 700 K; the faceted surface is covered by three-sided triangular pyramids with predominantly {1 1 2} surfaces. Che et al. [23] used the local density approximation (LDA) in first-principles calculations to examine why the above-mentioned overlayers preferentially induce faceting. They proposed that anisotropy of surface free energy is a necessary, but not sufficient condition for faceting. Kinetic factors (overcoming nucleation barriers, desorption energies) also play important roles in the faceting process. An empirical correlation between the overlayer Pauling electronegativities has also been previously

* Corresponding author. Tel.: +1-732-4455185; fax: +1-732-4454991.
E-mail address: madey@physics.rutgers.edu (T.E. Madey).

0368-2048/$ – see front matter © 2004 Elsevier B.V. All rights reserved.
doi:10.1016/j.elspec.2004.02.109

identified [6,7]. All the overlayers that induce faceting have Pauling electronegativities greater than 2.0, whereas metals that do not induce faceting of the substrate have Pauling electronegativities less than 2.0. Despite the empirical electronegativity correlation, Che and Chan [24] have shown recently using LDA that surface charging is not the governing factor in faceting. Consistent with the experiments of Tao et al. [18], they suggest that the governing factor is the specific chemical bonding between substrate and overlayer.

In systematic studies of metal overlayer films on W(1 1 1) with soft X-ray photoemission electron spectroscopy (SXPS), correlations have been found between the W $4f_{7/2}$ binding energy and the corresponding heat of adsorption of the adsorbate [18]. However, there is no clear correlation between the W $4f_{7/2}$ surface core-level shifts (SCLS) and Pauling electronegativity. This is consistent with the premise that while Pauling electronegativity is determined solely from initial state effects, both initial and final state effects affect the binding energy of a core-level electronic level. In recent SXPS studies of ultrathin transition metal films (Pd, Pt, Rh) on W(1 1 1) by Kolodziej et al. [25], it was clearly shown that a single monolayer of each of these metals "floats" on the surface of the W substrate, even as the surface faceting transition occurs. In comparison, for coverages exceeding 1 ML, atomic mixing at the interface and alloying are observed upon annealing.

To gain further understanding of the mechanisms associated with overlayer-induced faceting, an atomically rough surface of an fcc metal, Ir(2 1 0), was chosen for study. Brenner [26] has studied the formation of facets on iridium surfaces using field ion microscopy. He also showed that gaseous impurities could alter the rate of faceting and affect the activation energy needed for surface mass transport. The fcc (2 1 0) surface has a structure very similar to the bcc (1 1 1) except for an elongation along one of its axes. Recent studies by Ermanoski et al. [27] of Ir(2 1 0) have shown that oxygen induces faceting (i.e., nanometer-scale 3-sided pyramids with {3 1 1} and {1 1 0} sides) when the substrate is annealed to $T \geq 600$ K. Investigations into the reactivity of acetylene (C_2H_2) by Chen et al. [28] on both planar and faceted Ir(2 1 0) have revealed striking differences in the TPD spectra, indicating that the catalytic behaviour of the metal surface appears to be highly dependent upon its morphology.

Binding energy shifts of core electron states of surface atoms reflect chemical environments that are different from that of atoms in the bulk. The surface core-level shifts can provide a wealth of information on surface structure, alloying, intermixing, and adsorbate interactions. Before interpretation of chemical shifts is possible, however, knowledge of the origin of SCLSs is required.

By assuming complete screening for the core electron ionization process and using an equivalent core approximation, Johannson and Martensson [29] have predicted surface core-level shifts for the 5d transition metal series. Their results for surfaces of iridium reveal that all surface features experience binding energy shifts to smaller values than the bulk feature. Consistent with this theory, experimental evidence has been reported for SCLS to lower binding energies for different clean iridium surfaces such as (1 1 1), the 5×1 reconstruction of clean (0 0 1), and (1 0 0) 1×1 by van der Veen et al. [30]. In contrast, Barrett et al. [31] report experimental evidence for a subsurface layer SCLS to the *higher* binding energy side of the bulk peak for Ir(1 0 0) 1×1 and 5×1 reconstruction. This "inversion" in the core-level shift was supported by their use of tight binding calculations.

The presence of adsorbates on metal surfaces can significantly change the electronic properties of the surface atoms and subsequently induce binding energy shifts of core levels, which can reveal a multitude of information about the nature of bonding to metal surfaces. In this paper, we report studies in which interactions of the Ir(2 1 0) surface with the vacuum interface and with oxygen and hydrogen overlayers are probed. The clean Ir(2 1 0) spectrum reveals three surface features on the low binding energy side of the bulk feature; there is no evidence for surface/bulk peak "inversion". Adsorption of oxygen onto planar Ir(2 1 0) at room temperature causes a suppression of the surface features and an appearance of a new peak on the high binding energy of the bulk. Annealing in oxygen and cooling causes formation of pyramidal faceted structures on the surface containing {3 1 1} and {1 1 0} faces, as revealed by low energy electron diffraction (LEED) [27].

The SXPS spectra of the oxygen-covered planar and faceted Ir(2 1 0) surfaces are compared and although the normal emission spectra do not exhibit changes between the oxygen-covered planar and faceted surfaces, grazing emission spectra reveal significant contrast. SXPS spectra of clean, faceted Ir(2 1 0) are also presented.

2. Experimental

The experiments were performed in an ultrahigh vacuum (UHV) chamber, with base pressure lower than 1×10^{-10} Torr, (1 Torr = 133 Pa) on beamline U4A at the National Synchrotron Light Source. The photon energy used in most of this study was 110 eV with a nominal resolution of 90 meV. A VSW hemispherical energy analyzer having 100 mm mean radius and 5° angular acceptance angle collected the photoelectrons with a pass energy of 5 eV. This gives a nominal analyzer resolution of 90 meV, and a total instrumental resolution of approximately 127 meV. The photon flux was measured continuously and the XPS spectra shown here were normalized to account for gradually varying photon flux.

The samples were cleaned by repeated cycles of flash annealing in 1×10^{-7} Torr oxygen to ~2000 K and then by flashing to a similar temperature in UHV. This procedure was used at Rutgers on the same Ir(2 1 0) sample, where cleanliness was verified using TPD and AES [27]. The surface was characterized in situ using LEED and SXPS. The

temperature was measured using W5%Re–W26%Re thermocouple wires that were spot-welded to the rear of the iridium crystal. The faceted surface was generated by flashing the sample in 1×10^{-7} Torr oxygen and allowing it to cool to room temperature in oxygen. A clean faceted surface was generated by removal of oxygen at a low temperature via a surface chemical reaction. As reported elsewhere [27] the faceted surface is stable to $T \sim 600$ K and annealing in CO at $T \sim 550$ K can remove the oxygen completely, giving a clean faceted surface. Alternatively, annealing the faceted surface in H_2 (1×10^{-8} Torr) for 5 min at 470 K produces a clean, faceted surface.

At photon energies of ~110 eV, the Ir $4f_{7/2}$ photoemission signal is very surface sensitive and surface features exhibit relatively high intensity at normal emission. Different photon energies and different emission angles assist in the analysis of measured core levels, via their influence on the attenuation of features within the Ir $4f_{7/2}$ core-level spectra. (The emission angle is the angle between the surface normal and the axis of the analyzer lens system.) For example, higher photon energies provide more bulk information since the Ir $4f_{7/2}$ electrons have a larger kinetic energy, and a corresponding longer inelastic mean free path (escape depth) than electrons with lower kinetic energy. In this experiment, 180 eV photon energy was chosen to enhance the bulk feature. Grazing emission angles were adopted to provide enhanced surface information since at grazing angles, the electrons emitted from the bulk are more effectively attenuated than the electron signal from the near surface layers. The grazing emission angle used in this experiment is 70° from the surface normal. In this study, the analysis of Ir $4f_{7/2}$ core-level photoemission spectra involved a non-linear least squares fitting procedure and Doniach–Sunjic lineshapes, which have been used elsewhere for the W $4f_{7/2}$ core-level feature [18,19,25,32]. The parameters used with this lineshape were Lorentzian linewidth, Gaussian linewidth, and the lineshape asymmetry α parameter; the latter is a measure of the effects of electron/hole pair creation during photoemission.

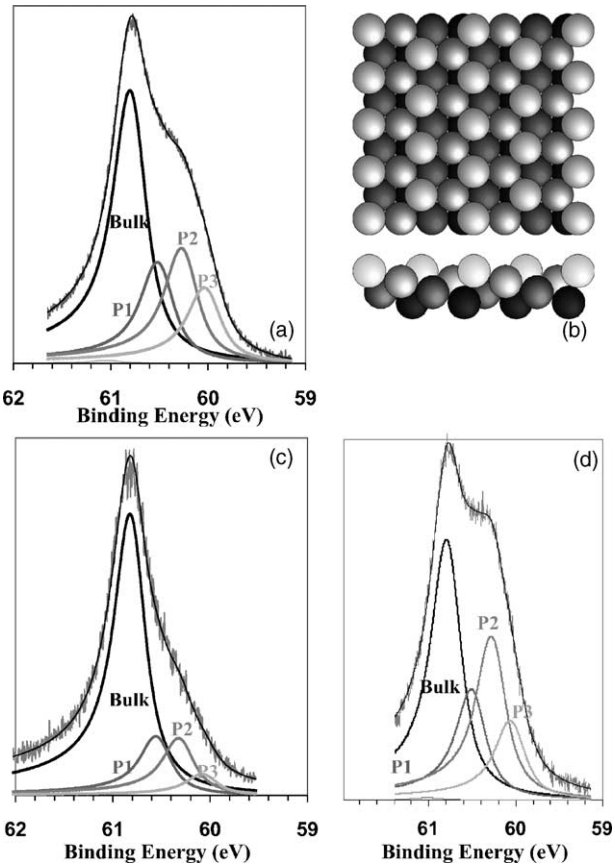

Fig. 1. (a): Ir $4f_{7/2}$ spectum for clean Ir(2 1 0) at normal emission for a photon energy of 110 eV. The spectra is fitted with four peaks each having a linewidth of 300 meV, a Gaussian width of 150 meV, and a symmetry parameter $\alpha = 0.121$. The three surface peaks, labeled P1, P2, and P3 correspond to the first, second and third layers and have core-level shifts of −281, −529, and −765 meV, respectively. (b): Schematic of unrelaxed Ir(2 1 0) surface illustrating (a) top side (b) side views. Note there are four layers exposed to the vacuum [36]. (c): Ir $4f_{7/2}$ spectrum for clean Ir(2 1 0) at normal emission for a photon energy of 180 eV. The surface features are attenuated significantly allowing a more exact identification of the bulk intensity feature characteristics. (d): Ir $4f_{7/2}$ grazing emission spectrum at 110 eV revealing increased surface/bulk ratio due to an increase in bulk attenuation. Emission angle 70° with respect to normal.

3. Results

A typical Ir $4f_{7/2}$ spectrum for clean Ir(2 1 0) is shown in Fig. 1a for a photon energy of 110 eV. In attempting to fit this spectrum, several constraints were imposed. First, the full linewidth of any one feature was assumed to be ~300 meV, as observed in previous investigations [30,31]. With this constraint a minimum of four features were needed to fit the data. Based on the model of Fig. 1b, this requirement can be physically justified: three surface features from surface layers that interact with the vacuum interface plus the bulk feature (note that the numbers of nearest neighbors for atoms in the top four layers of Ir(2 1 0) are 6, 9, 11, and 12, respectively, so that the fourth layer has bulk coordination). It is not necessary to include additional features in fitting the data, indicating that any signal from the fourth layer below the surface, shown in Fig. 1b, is encompassed by the large bulk feature. To verify the assignment of surface and bulk components a higher photon energy of 180 eV was used to enhance the bulk feature (Fig. 1c); grazing emission (Fig. 1d) at 110 eV was used to enhance the surface features. All three spectra (Fig. 1a, c and d) were fit with four peaks having the same binding energies in each spectrum. The changes in relative intensity between normal and grazing emission allow us to conclude that the three smaller features at lower binding energy are surface features. Note that Fig. 1c reveals a 55% decrease in surface/bulk ratio, which provides adequate determination of the core-level parameters. The optimal fit, i.e. smallest deviation between experiment and fitted spectrum, was found with bulk parameters of 63.8 eV binding energy, an asymmetry parameter of 0.121, Lorentzian linewidth of 300 meV, and Gaussian width

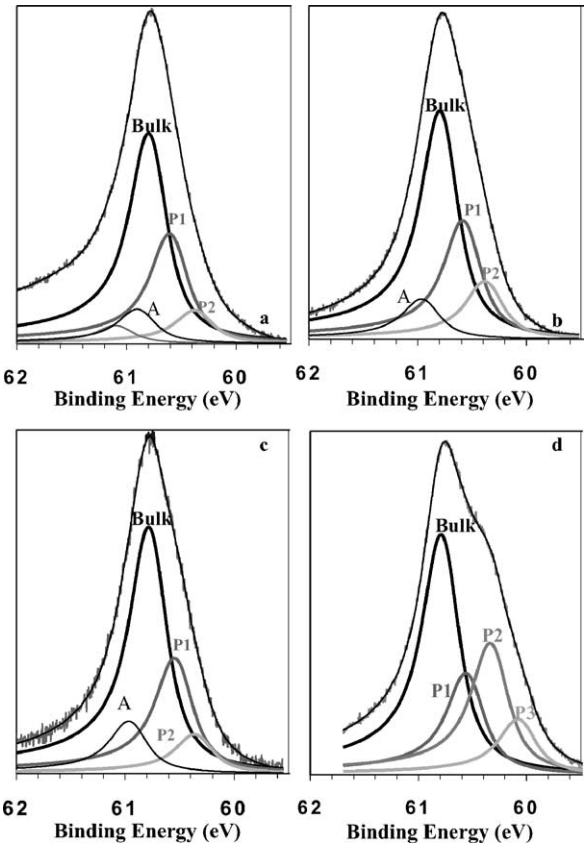

Fig. 2. (a): Ir $4f_{7/2}$ spectrum for oxygen-covered planar Ir(2 1 0), illustrating the considerable suppression of the surface features. The suppression is accompanied by a core-level shift toward the bulk feature. Two features (A and B) on the high binding energy side of the bulk peak arise with binding energy shifts of 190 and 420 meV. (b): Ir $4f_{7/2}$ spectrum at normal emission for oxygen-covered faceted Ir(2 1 0) showing little deviation from (a). (c): $Ir_{4/7}$ spectrum at grazing emission for oxygen-covered faceted Ir(2 1 0); compare to (b). (d): Ir $4f_{7/2}$ spectra at normal emission for clean faceted Ir(2 1 0) revealing surface features with core-level shifts of −230, −454, and −710 meV.

of 150 meV. The grazing emission spectrum in Fig. 1d produced a 28% increase of the surface features with respect to the bulk. Least squares fits of the spectra of Fig. 1 revealed surface core-level binding energy shifts of −765, −529, and −281 meV for the first, second and third layer peaks, respectively, measured with respect to the bulk peak.

Fig. 2a shows the Ir $4f_{7/2}$ spectrum following oxygen deposition on the planar Ir(2 1 0) surface. A significant suppression of the surface features is observed on the low binding energy side of the bulk peak, which is notably the dominant feature in the spectrum. Furthermore, the surface features have been shifted to higher binding energies relative to those of the clean surface, as a consequence of the interaction with the oxygen at the surface. The high binding energy peaks have SCLSs of 192 and 420 meV from the bulk feature. If we consider the structure of the fcc (2 1 0) surface (Fig. 1b), it appears that oxygen interacts initially with the first and second layers, which are subject to the greatest binding energy shift. This could give rise to an oxygen-induced inversion of the surface core-level shifts, and based on the data in Fig. 1d it seems very likely that the first layer does not have the minimum binding energy of the components shown in the clean spectrum of Fig. 1a. The parameters optimized for the bulk peak in the oxygen-covered surface were the same (within experimental error) as the parameters found in the clean analysis (Fig. 1a–d). An additional feature is prominent in the spectrum of Fig. 2a for the oxygen-covered surface, labeled A on the high binding energy side of the bulk peak. (The small peak B may be a consequence of the linear background subtraction). These peaks are associated with the surface iridium layer interacting with the oxygen overlayer, leading to a shift in binding energy higher than the bulk. Such core-level shifts are often seen for oxygen adsorption on metal substrates [33–38]. The surface/bulk ratio changes from normal to grazing emission for this system reveal an increase of 10% for both low binding energy features, with peak A increasing by 54% and B remaining constant.

Fig. 2b shows the core-level spectrum at normal emission of the oxygen-covered faceted Ir(2 1 0) as characterized by LEED in Fig. 3. No striking differences in the SXPS data are observed for the oxygen-covered planar and faceted surfaces. This is surprising since the faces of the pyramids are {3 1 1} and {1 1 0}, and are expected to have different surface layers contributing to the spectra [27]. Oxygen should also play a role in suppressing the surface components. However, at normal emission, the slopes of the facet (∼20°) faces should not significantly affect the surface-to-bulk $4f_{7/2}$ intensity ratio. The LEED pattern in Fig. 3 is typical for the faceted Ir(2 1 0) surface. LEED beams scattered by a faceted substrate do not move radially to and from the (0 0) beam when the energy is changed. Instead, the beams scattered from a faceted surface converge on points corresponding to specular reflections from the facet planes. LEED patterns from faceted surfaces are described in more detail by Song et al. [39,40] for W(1 1 1) and by Ermanoski et al. [27] for Ir(2 1 0). The SXPS spectrum of oxygen-covered faceted Ir(2 1 0) at grazing emission is shown in Fig. 2c. The changes in surface/bulk intensity ratio from normal to grazing emission (compare Fig. 2b and c) for the oxygen-covered faceted Ir(2 1 0) system reveal dramatic variations from the oxygen-covered planar Ir(2 1 0) surface. From normal to grazing, the low binding energy features (labeled P1 and P2) are found to decrease by 10 and 60%, respectively, while the lone high binding energy peak labeled A increases by 20%.

Fig. 2d shows the Ir $4_{7/2}$ spectrum for the clean, faceted Ir(2 1 0) surface. This $4f_{7/2}$ spectrum is narrower than that for the clean, planar Ir(2 1 0) surface (Fig. 1a). Using the same process as used to fit the clean, planar Ir(2 1 0) spectrum in Fig. 1a, three surface layer contributions are present in the spectrum of Fig. 2d, but with smaller binding energy shifts than those exhibited for the clean planar surface. This smaller core-level shift is associated with different atomic packing density for {1 1 0} and {3 1 1} facets, as compared to the atomically rough (2 1 0) surface. The surface layers

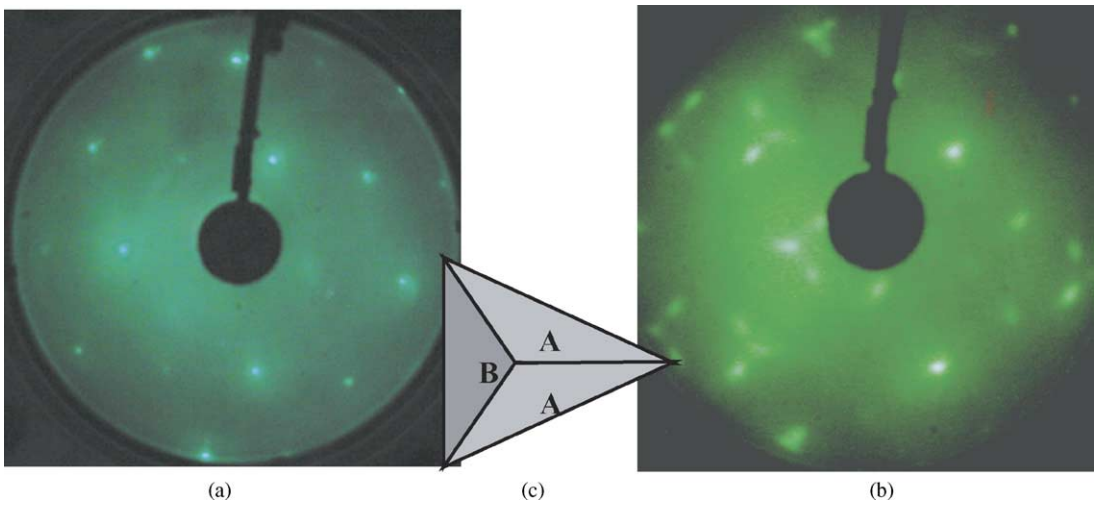

Fig. 3. LEED patterns for (a) clean, planar Ir(2 1 0) at $E_e = 150$ eV, and (b) oxygen-faceted Ir(2 1 0) at $E_e = 250$ eV. Note the characteristic three facet spots in a triangular pattern surrounding the clean (1×1) spots. (c) Schematic representation of a three-sided iridium facet structure induced by annealing (2 1 0) surface in oxygen; A facets have {3 1 1} orientation, and B facet is {1 1 0}.

labeled A, B, C have core-level shifts of −230, −450, and −710 meV respectively.

4. Discussion

Table 1 summarizes the results for the surface core-level shifts and the surface/bulk ratio changes from normal to grazing for clean planar Ir(2 1 0), oxygen on planar Ir(2 1 0), oxygen on faceted Ir, and for a clean faceted iridium surface. Fig. 1a–d allow us to conclude that the clean Ir(2 1 0) spectra exhibit surface core-level features that have lower binding energies than the observed bulk feature. The surface features have an average core-level shift of −325 meV from the bulk. Measurement of the surface to bulk ratio differences indicate that peaks P1, P2, and P3 increase by 18, 54, and 14%, respectively, from normal emission to grazing emission. It is often found that peaks with largest core-level shift are associated with the topmost atomic layer, and peaks with smaller shifts are attributed to subsurface layers. The smaller the binding energy shift, the deeper the layer until the layers are covered by the topmost surface layer and produce the bulk signal. However, Lizzit et al. [41] have shown experimentally and with first-principles theory that the largest shift observed for Be(10$\bar{1}$0) is associated with the second (subsurface) layer and not the surface layer. This inversion between the first and second layer is attributed to the complex interplay between initial and final state effects that may also play a role in other clean metal surfaces. The fact that the intensity of P2 increases by such a dramatic amount demonstrates the possibility that such an inversion occurs in Ir 4f features associated with the surface atomic layers. Another possible explanation for the large P2 feature in Fig. 1a is that forward focusing occurs along a low-index direction at grazing emission. However, for our experimental configuration, there are no low-index directions (i.e. no directions containing rows of nearest-neighbor or next-nearest neighbor atoms) at grazing emission detection, which corresponds approximately to the [1 3 5] direction.

The intensities of the Ir 4f surface features at normal emission also change with photon energy (Fig. 1a and c). For $h\nu = 180$ eV, the electron attenuation length of the photoemitted electrons is (relatively) large, and the bulk peak is considerably more intense than the surface peaks (the P3, P2, and P1 intensities are 6.7, 20, and 21% of the bulk intensity, respectively). For $h\nu = 110$ eV the electron attenuation length is smaller than for 180 eV and the surface peaks are more prominent (29, 44, and 37% of the bulk peak, respectively). Moreover, at 180 eV, one might expect that the relative intensities of P3, P2, and P1 represent

Table 1
Surface core-level shifts and surface/bulk ratio changes for differently-prepared iridium (2 1 0) surfaces

Iridium surface	Surface core-level shifts (meV)					Surface/bulk ratio, grazing percent change from normal
	B	A	P1	P2	P3	
Clean planar (2 1 0)	N/A	N/A	−299	−513	−725	P1 = 18%, P2 = 54%, P3 = 14%
Oxygen on planar (2 1 0)	420	192	−155	−345	N/A	B = 0%, A = 54%, P1, P2 = 10%,
Oxygen on faceted surface	N/A	195	−160	−360	N/A	A = 20%, P1 = −10%, P2 = −60%
Clean faceted surface	N/A	N/A	−230	−450	−710	P1 = −13%, P2 = 32%, P3 = −3.2%

(roughly) the relative surface concentrations, and that they should have more-or-less equal intensity. A possible reason for the energy-dependent intensities of the surface features in Fig. 1a and c may involve photoelectron diffraction [42]; in the energy range of the present experiments (electron kinetic energies of ∼50–120 eV) there is considerable structure in the angular dependence of the elastic scattering factor for metal atoms [43]. The implication is that diffraction may lead to an energy-dependent modulation of the electron emission intensity as a function of detection angle. This is a point that requires further study before a firm conclusion can be reached.

The negative binding energy shift of the surface features for Ir(2 1 0) is consistent with the theoretical predictions of Johannson and Martensson [29] and the experimental evidence of van der Veen et al. [30] for Ir(1 1 1) and Ir(1 0 0) surfaces. As mentioned earlier, Barrett et al. [31] more recently reported that the surface and subsurface Ir $4f_{7/2}$ features on Ir(1 0 0) are displaced from the bulk peak with both lower and higher binding energy values, respectively. Our inspection of the data by Barrett et al. reveals considerable deviation between the raw data and the fitted peaks; perhaps an improved fit could change the interpretation of their results.

Surface core-level shifts in iridium have been mainly attributed to rehybridization of the s, p and d orbitals, d-band narrowing, and changes in surface states [44]. The core-level shift to the lower binding energy side of the bulk feature establishes that the core electrons are more weakly bound at the surface than in the bulk; this is understood by comparing the initial and final states of the surface and bulk atoms. The final state represents the core-ionized atom, with the valence charge distribution essentially that of a $(Z+1)$ element for a Z metal [30]. For Ir, the $(Z+1)$ screening involves the anti-bonding part of the d-band and the bonding due to the conduction electrons is weaker in the final state than in the initial state [29]. However, the use of the $(Z+1)$ model alone has been shown by Andersen et al. [45] to introduce a variance of typically 100 meV for most 4d elements due to errors in values used for the relaxation of the first layer. Andersen et al. also conclude that the simple d-band narrowing model does not always predict correct SCLSs.

Dosing of planar Ir(2 1 0) with oxygen (Fig. 2a) produces a significant suppression of intensity and positive binding energy shifts in the surface core levels. The oxygen-induced faceting of iridium is reminiscent of the morphological changes accompanying oxygen-induced faceting of W(1 1 1) [1,2]. Furthermore, similarities exist between surface core-level shifts observed for oxygen-covered W and Ir. Indeed, a number of investigators have reported observations of positive surface core-level shifts for oxygen-covered metal surfaces [34–38]. Oguchi [36] investigated the SCLS of the (1 × 1) oxygen-covered W(1 1 0) surface using the all-electron atomic force FLAPW method within the local density approximation. Oxygen causes the binding energy of the 4f core levels of the surface W atoms to increase by 0.73 eV with respect to the bulk W atoms with an average increase of 1 eV from the clean surface W atom binding energy. The core-level binding energy of iridium surface atoms (peak A) is shifted through the introduction of oxygen by 0.2 eV with respect to the bulk Ir atoms. This corresponds to an average shift of 0.7 eV from the clean Ir surface atom binding energy (average surface binding energy shift: ∼−525 meV) which is similar to the shift observed with O/W(1 1 0). The (1 × 1)-O overlayer observed on the W(1 1 0) surface enhances the positive binding energy shift due to oxygen atoms interacting with equivalent W atoms on the surface. We suggest that similar oxygen-induced effects may occur for iridium surface atoms. Oguchi concluded the SCLSs are due predominately to the difference in the Madelung potential between the surface and bulk sites. Charge transfer (intra-atomic potential) alone could not explain the observed SCLSs. Using the Weinert and Watson [46] prescription, an extra-atomic term (potential due to other charges) combined with the intra-atomic term produces SCLSs that are comparable with experimental results.

Comparison of the oxygen-covered faceted (Fig. 2b) and planar (Fig. 2a) Ir(2 1 0) normal emission spectra reveals little difference. Oxygen suppresses the features in both spectra and few differences are observed, even though the planar and faceted surfaces are quite different morphologically. In addition, van der Veen et al. [30] have shown that adsorbate-induced SCLSs are also sensitive to changes in structural properties of the substrate. The oxygen suppresses the intensity of the surface features more than the bulk feature at a photon energy of 110 eV. This is different from Ir $4f_{7/2}$ spectra accompanying the deposition of Au or Pd on Ir: Au and Pd overlayers attenuate bulk and surface features equally without changing SCLSs [47].

Hydrogen covered surfaces have also been recently investigated, partly because of their relevance to the electronic device industry [48–50]. For Ir(2 1 0), adsorption of hydrogen causes negligible binding energy shifts of the surface Ir atoms. A hydrogen saturated surface (∼0.5 ML [28]) gives a SXPS spectrum very similar to the clean planar Ir(2 1 0) $4f_{7/2}$ spectra shown in Fig. 1a. This result is in contrast to other hydrogenated metal surfaces. Jupille et al. [49] reported significant hydrogen-induced binding energy shifts of W $4f_{7/2}$ core levels for the W(1 0 0) surface. In fact, suppression and shifting of W $4f_{7/2}$ surface features are observed with a very small (0.06 Langmuir) dose of H_2 on W(1 1 2) [47].

Following the introduction of H_2 and the removal of oxygen from the oxygen-covered faceted Ir(2 1 0) surface [27], the clean faceted surface is generated and the suppressed features on the low binding energy side of the bulk become visible. The three peaks labeled P1, P2, and P3 in Fig. 2d have smaller core-level shifts than similar features in the clean planar Ir(2 1 0) spectum of Fig. 1a. Fig. 3c shows a schematic of a typical pyramid produced on an oxygen-induced faceted Ir(2 1 0) surface. As indicated in Fig. 3c faceted features on Ir(2 1 0) are not three-fold symmetric as on the bcc (1 1 1)

surface of W, but exhibit two-fold symmetry as elongated pyramids, in which two sides of the pyramid are identical, labeled A, and the third B is a different planar orientation. The two distinct faces A and B dominate the observed clean, faceted Ir(2 1 0) spectrum. Ermanoski et al. [27] have used LEED to determine faces A to be {3 1 1}, and face B to be {1 1 0}. Including the clean planar Ir(2 1 0) surface shown in Fig. 1a, we observe four surfaces that produce surface core-level shifts on the lower binding energy side of the bulk, i.e., all surfaces observed have surface Ir atoms for which core-level binding energies are smaller than for bulk atoms. A comparison of the normal and grazing incidence data reveals that features labeled P1 and P3 (Fig. 2) decrease in surface/bulk ratio by 13 and 3.2%, respectively while P2 increases by 32%. The peak labeled P2 is most likely from one of the faces marked A in Fig. 3c. Unfortunately, the orientation of the pyramids with respect to the incident beam and the analyzer axis was not controlled, and it was not possible to rotate the azimuth of the sample in the U4A chamber to align one of the faces normal to the analyzer to get normal emission. Nevertheless, it is clear that both clean, planar and clean, faceted Ir(2 1 0) surfaces exhibit SCLSs to lower binding energy.

5. Conclusion

Based on measurements of clean Ir(2 1 0) $4f_{7/2}$ spectra it has been determined that all surface features are shifted to the low binding energy side of the bulk feature, consistent with previous results for Ir(1 0 0) (1 × 1) and (5 × 1) and Ir(1 1 1) [30], and contrary to data of Barrett et. al [31]. Ir $4f_{7/2}$ level shifts with respect to the bulk of −765, −529, and −281 meV are associated with the first, second and third layer of Ir atoms, respectively. Oxygen-covered planar Ir(2 1 0) and oxygen-covered, faceted Ir(2 1 0) $4f_{7/2}$ spectra are compared and found to be very similar with the exception of an extra feature on the high binding energy side of the bulk peak. Both oxygen-covered surfaces reveal a distinct suppression of the surface features with an additional binding energy shift toward the bulk peak. A comparison of the grazing emission spectra for these two systems reveals substantial differences in the topmost surface layer structure. The Ir $4f_{7/2}$ spectra for the clean, faceted Ir(2 1 0) have been measured and the surface core-level shifts are slightly different from those of the clean planar Ir(2 1 0) surfaces with values of −230, −450, and −710 meV. The removal of oxygen from both the planar and faceted Ir(2 1 0) surfaces is achieved by reaction with hydrogen, and no binding energy shift is observed for a hydrogen covered iridium surface.

Acknowledgements

This work has been supported in part by the U.S. Army Research Office and the U.S. Department of Energy. M.J. Gladys acknowledges support from the Australian-American Fulbright Association. The National Synchrotron Light Source at Brookhaven National Laboratory is supported by the U.S. Department of Energy, Division of Materials Sciences and Division of Chemical Sciences (DOE Contract No. DOE-AC02-76CH00016).

References

[1] N.J. Taylor, Surf. Sci. 2 (1964) 544.
[2] J.C. Tracy, J.M. Blakely, Surf. Sci. 13 (1968) 313.
[3] A. Cetronio, J.P. Jones, Surf. Sci. 40 (1973) 227.
[4] F. Bonczec, T. Engel, E. Bauer, Surf. Sci. 97 (1980) 595.
[5] E. Bauer, in: D.A. King, D.P. Woodruff (Eds.), Chemical Physics of Solid Surfaces and Heterogeneous Catalysis, vol. 3B, Elsevier, New York, 1984, p. 1.
[6] T.E. Madey, J. Guan, C.-Z. Dong, S.M. Shivaprasad, Surf. Sci. 287/288 (1993) 826.
[7] T.E. Madey, J. Guan, C.-H. Nien, C.-Z. Dong, H.-S. Tao, R.A. Campbell, Surf. Rev. Lett. 3 (1996) 1315.
[8] T.E. Madey, K. Pelhos, Q. Wu, R. Barnes, I. Ermanoski, W. Chen, J.J. Kolodziej, J.E. Rowe, Proc. Natl. Acad. Sci. 99 (2002) 6503.
[9] C. Zhang, M.A. van Hove, G.A. Somorjai, Surf. Sci. 149 (1985) 326.
[10] J. Guan, R.A. Campbell, T.E. Madey, J. Vac. Sci. Technol. A 13 (1995) 1484.
[11] K.-J. Song, J.C. Lin, M.Y. Lai, Y.L. Wang, Surf. Sci. 327 (1995) 17.
[12] M. Sander, R. Imbihl, R. Schuster, J.V. Barth, G. ErtlSurf. Sci. 271 (1992) 159.
[13] R.E. Kuby, C.S. McKee, M.W. Roberts, Surf. Sci. 55 (1976) 725.
[14] R.E. Kuby, C.S. McKee, L.V. Renny, Surf. Sci. 97 (1980) 725.
[15] P.J. Knight, S.M. Driver, D.P. Woodruff, Surf. Sci. 376 (1997) 374.
[16] S. Reiter, E. Taglauer, Surf. Sci. 367 (1996) 33.
[17] E. Taglauer, S. Reiter, A. Liegl, S. Schomann, Nucl. Instrum. Methods B 118 (1996) 456.
[18] H.-S. Tao, T.E. Madey, J.E. Rowe, Surf. Sci. 407 (1998) L640.
[19] J.J. Kolodziej, K. Pelhos, I.M. Abdelrehim, J.W. Keister, J.E. Rowe, T.E. Madey, Prog. Surf. Sci. 59 (1999) 117.
[20] M. Gladys, G. Jackson, J.E. Rowe, T.E. Madey, Surf. Sci. 544 (2003) 193.
[21] J. Guan, R.A. Gampbell, T.E. Madey, Surf. Sci. 341 (1995) 311.
[22] J. Kolaczkiewicz, E. Bauer, Surf. Sci. 420 (1999) 157.
[23] J.G. Che, C.T. Chan, C.H. Kuo, T.C. Leung, Phys. Rev. Lett. 79 (1997) 4230.
[24] J.G. Che, C.T. Chan, Phys. Rev. B 67 (2003) 125411.
[25] J.J. Kolodziej, T.E. Madey, J.W. Keister, J.E. Rowe, Phys. Rev. B 65 (2002) 075413.
[26] S.S. Brenner, Surf. Sci. 2 (1964) 496.
[27] I. Ermanoski, K. Pelhos, J.S. Quinton, W. Chen, T.E. Madey, Surf. Sci. 549 (2004) 1.
[28] W. Chen, I. Ermanoski, Q. Wu, T.E. Madey, H.H. Hwu, J.G. Chen, J. Phys. Chem. B 107 (2003) 5231.
[29] B. Johansson, N. Martensson, Helv. Phys. Acta 56 (1983) 405.
[30] F.J. Van der Veen, F. Himpsel, D. Eastman, Phys. Rev. Lett. 44 (1980) 189.
[31] N. Barrett, C. Guillot, B. Villette, G. Tréglia, B. Legrand, Surf. Sci. 251/252 (1991) 717.
[32] S. Doniach, M. Sunjic, J. Phys. C. 3 (1970) 285.
[33] S. Lizzit, A. Baraldi, A. Groso, K. Reuter, M.V. Ganduglia-Pirovano, C. Stampl, M. Scheffler, M. Stichler, C. Keller, W. Wurth, D. Menzel, Phys. Rev. B 63 (2001) 205419.
[34] K. Prince, A. Santoni, A. Morgante, G. Comelli, Surf. Sci. 317 (1994) 397.

[35] K. Park, G. Simmons, K. Klier, Surf. Sci. 367 (1996) 307.
[36] T. Oguchi, Surf. Sci. 438 (1999) 37.
[37] G. Abramovici, M. Desjonqueres, D. Spanjaard, J. Phys. I 5 (1995) 907.
[38] O. Bjorneholm, A. Nilsson, H. Tillborg, P. Bennich, A. Sandell, B. Hernnäs, C. Puglia, N. Mårtensson, Surf. Sci. 315 (1994) L983.
[39] K.-J. Song, C.-Z. Dong, T.E. Madey, Langmuir 7 (1991) 3019.
[40] K.-J. Song, R.E. Demmin, C.-Z. Dong, E. Garfunkel, T.E. Madey, Surf. Sci. 227 (1990) L79.
[41] S. Lizzit, K. Pohl, A. Baraldi, G. Comelli, V. Fritzsche, E.W. Plummer, R. Stumpf, P. Hofmann, Phys. Rev. Lett. 81 (1998) 3271.
[42] C. Westphal, Surf. Sci. Rep. 50 (2003) 1–106.
[43] A. Jablonski, F. Salvat, C.J. Powell, NIST Electron Elastic-Scattering Cross-Section Database—Version 3.0, National Institute of Standards and Technology, Gaithersburg, MD, 2002.
[44] J.J. Kolodziej, T.E. Madey, J.W. Keister, J.E. Rowe, Phys. Rev. B 62 (2000) 5150.
[45] J.N. Andersen, D. Hennig, E. Lundgren, M. Methfessel, R. Nyholm, M. Scheffler, Phys. Rev. B 50 (1994) 17525.
[46] M. Weinert, R. Watson, Phys. Rev. B 51 (1995) 17168.
[47] H.-S. Tao, J.E. Rowe, T.E. Madey, unpublished data.
[48] L. Ley, R. Graupner, J.B. Cui, J. Ristein, Carbon 37 (1999) 793.
[49] J. Jupille, K. Purcell, D. King, Surf. Sci. 367 (1996) 149.
[50] S. Scholz, K. Jacobi, Phys. Rev. B 52 (1995) 5795.